An analysis of $1.55\ \mu m$ InAs / InP quantum dash lasers

S. C. Heck, S. B. Healy, S. Osborne' , E. P. O'Reilly, F. Lelarge, F. Poingt, A. Accard, F. Pommereau, O. Le Gouezigou, and B. Dagens

Citation: Appl. Phys. Lett. **92**, 251105 (2008); doi: 10.1063/1.2952194
View online: http://dx.doi.org/10.1063/1.2952194
View Table of Contents: http://aip.scitation.org/toc/apl/92/25
Published by the American Institute of Physics

An analysis of 1.55 μm InAs/InP quantum dash lasers

S. C. Heck,[1,2] S. B. Healy,[1] S. Osborne,[1,a)] E. P. O'Reilly,[1,2] F. Lelarge,[3] F. Poingt,[3] A. Accard,[3] F. Pommereau,[3] O. Le Gouezigou,[3] and B. Dagens[3]
[1]*Tyndall National Institute, Lee Maltings, Cork, Ireland*
[2]*Department of Physics, University College Cork, Ireland*
[3]*Alcatel Thales III-V Laboratory, R.D.128, 91767 Palaiseau, France*

(Received 24 April 2008; accepted 5 June 2008; published online 24 June 2008)

Calculations show that electron states are not confined in the dashes in 1.55 μm InAs/InP quantum dash-in-a-well laser structures. The combination of strain and three-dimensional confinement reduces the calculated density of states (DOS) near the valence band maximum, with the conduction and valence DOS then almost equal close to the band edges. Calculations and photoabsorption measurements show strongly polarized spontaneous emission and gain spectra. Experimental analysis shows the room temperature threshold current is dominated by nonradiative current paths. © *2008 American Institute of Physics*. [DOI: 10.1063/1.2952194]

There is a strong interest in quantum dots because of their potential benefits such as a lower and temperature insensitive threshold current compared with quantum well lasers. GaAs-based 1.3 μm quantum dot lasers have been widely studied[1] and are now commercially available. Because it is difficult to extend GaAs-based materials to the second telecommunications window, around 1.5 μm, InAs quantum dots grown on InP substrates represent a promising alternative. In practice, growth on the commercially favored (001) oriented InP substrates results in elongated quantum dots, called quantum dashes.[2] These InAs/InP quantum dash lasers have demonstrated many impressive characteristics[2] such as high modal gain per dash layer and high characteristic temperature, T_0.

In this letter, we analyze the effect of quantum confinement and strain on the properties of quantum dash lasers. Eight-band $\mathbf{k}\cdot\mathbf{p}$ calculations are undertaken to determine the band structure and the polarization dependence of optical recombination near the band edge.[3–6] We find, due to the different localization of electrons and holes, the valence band (VB) and conduction band (CB) edge density of states (DOS) can be of comparable magnitude, close to the ideal band structure for a semiconductor laser.[7] The combination of strain and dash shape leads to the optical matrix elements being strongly enhanced for light polarized parallel to the dash long axis.[8] We use a combination of edge-photovoltage (E-PV) and spontaneous emission (SE) measurements to confirm the strong polarization anistropy. Previous studies have shown that nonradiative losses due to Auger recombination dominate the room temperature threshold current and influence the values of T_0 in 1.5 μm InP-based lasers.[9,10] The experimental analysis presented here shows that, despite the beneficial band structure, this is also the case for 1.5 μm InGaAsP quantum dash structures.

The lasers studied here are InAs dash-in-a-well (DWELL) devices. The dashes are confined within a 6 nm lattice-matched InGaAsP quantum well (band gap 0.855 eV), embedded in a lattice-matched InGaAsP barrier (band gap 1.05 eV). For the theoretical work, we assume a 1.3 nm high InAs dash with base length 15 nm $\times$ 80 nm to give emission at 1.55 μm, with a dash density per layer of 2×10^{10} cm^{-2}. The left inset in Fig. 1 shows a schematic of the dash, with the long axis along the (1-10) crystallographic axis, and the shorter in-plane axis along (110). The laser cavity is parallel to the (110) direction. The right inset in Fig. 1 shows the different polarization directions studied below. The lasers used in the experimental work are fabricated into buried-heterostructure devices (see Ref. 2 for more information).

Figure 1 shows the band offsets, calculated as in Ref. 11, and lowest confined state energies for the InAs DWELL structure considered. We find that the lowest electron state is not confined in the InAs dash due to the low electron mass and small CB offset. By contrast, the heavy holes (defined along the growth direction) experience a deep potential, and are well confined within the dash. The light holes are calculated to have nearly no offset between the dash and the well, with the highest valence state with significant light-hole character then found to be in the well (Fig. 1). Figure 2 shows the absorption spectrum for light polarized along each of the three axes of a quantum dash, calculated for all transitions between states within 120 meV of the CB edge and

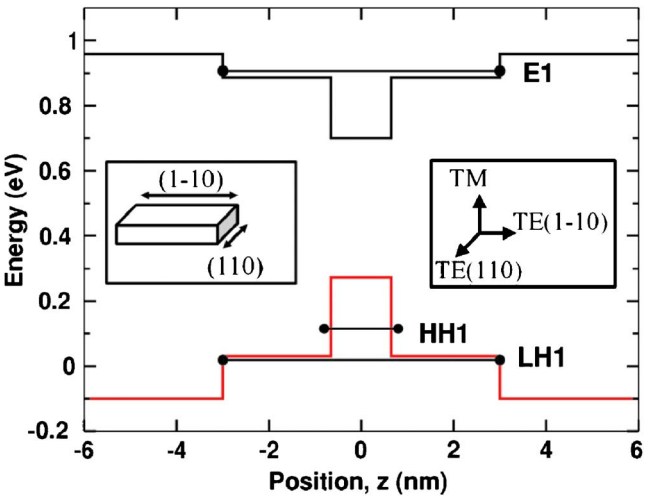

FIG. 1. (Color online) Calculated conduction and heavy hole band edges through the center of a DWELL. The lines with circles at the end show the calculated electron and heavy hole ground state energies, and the highest light-holelike valence state. The left inset shows a schematic diagram of the dash with the dash long axis along (1-10) and the short axis along (110). The right inset shows the axes of polarization.

a)Electronic mail: simon.osborne@tyndall.ie.

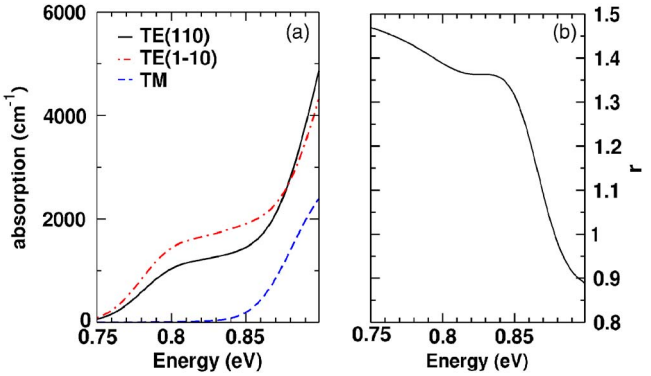

FIG. 2. (Color online) (a) Calculated TE(110)- (black solid), TE(1-10)- (red dashed dotted), and TM-polarized (blue dashed) absorption spectra and (b) ratio $r=|M_T^{(1-10)}|^2/|M_T^{(110)}|^2$ squared transition matrix elements.

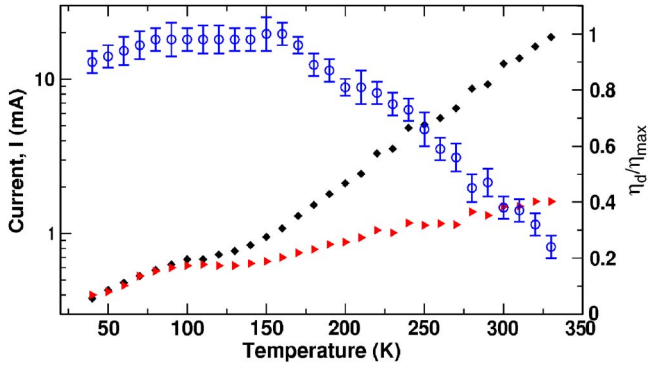

FIG. 4. (Color online) Left axis: plot of total threshold current (filled black diamonds) and total radiative contribution to threshold (filled red triangles) as a function of temperature. Right axis: Normalized external differential quantum efficiency (open blue circles) for a DWELL laser.

100 meV of the VB edge and includes a Gaussian broadening of 20 meV. We see a strong suppression of TM emission near the optical gap since TM polarized recombination is predominantly associated with transitions between electron and light-hole states. In addition, the asymmetry of the dash base dimensions reduces the symmetry of the highest confined valence states, leading to an enhanced transition matrix element and absorption coefficient for light polarized in the (1-10) direction relative to that for the (110) direction. We calculate that the ratio of the (1-10) to (110) squared transition matrix elements $r=|M_T^{(1-10)}|^2/|M_T^{(110)}|^2\approx 1.45$ for the lowest energy transition, and remains above 1.00 for all transitions below the well edge at 0.855 eV [see Fig. 2(b)]. This anistropy benefits the laser operation: the gain is maximized for light polarized along the (1-10) direction, and there is a reduction in the SE in the (110) direction, leading to a reduction in the total radiative current required to reach laser threshold.

We verify our calculations with a combination of E-PV and SE measurements and calibrate spectra with orthogonal polarizations using the technique introduced in Ref. 12. The E-PV spectra for the TE(1-10) and TM polarizations are shown in Fig. 3(a). We see that the TM absorption is weak over an energy range of at least 50 meV, in agreement with theory. We also measured the polarized SE from a window

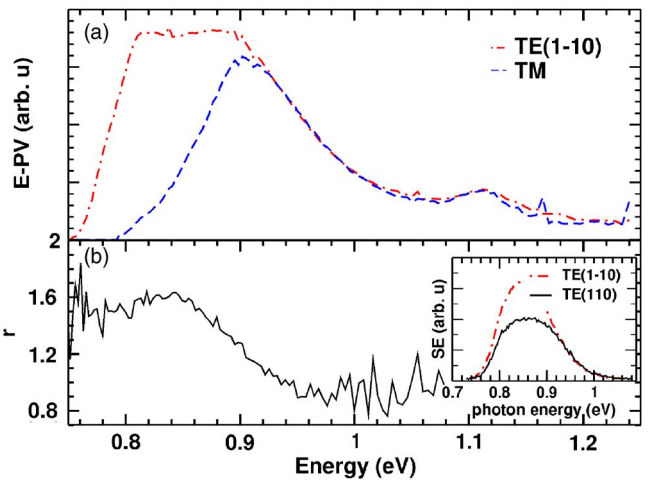

FIG. 3. (Color online) (a) TE(1-10) (red dashed-dotted) and TM (blue dashed) photovoltage spectra for DWELL laser sample. (b) Measured ratio of TE(1-10) (red dashed-dotted) to TE(110) (black solid) SE spectra. (Inset) Polarized SE spectra.

fabricated into the top contact of the laser. The inset in Fig. 3(b) confirms that the (1-10) polarized SE is enhanced with respect to the (110) emission. In this case, the ratio $r=|M_T^{(1-10)}|^2/|M_T^{(110)}|^2$ can be obtained by dividing the (1-10) SE spectrum by the (110) one, and is shown in Fig. 3(b). The measured ratio is close to 1.5 for photon energies up to 0.85 eV, then decreases to close to unity, in agreement with the theoretical results in Fig. 2.

An ideal semiconductor laser should have a small and equal DOS in the CB and in the VB, to minimize the transparency carrier density and maximize the differential gain.[7] In the best quantum well or dot lasers, this is not achieved because the CB DOS is always smaller than the valence DOS. However, the difference in confinement dimension for electrons and holes, combined with the large strain-induced VB splitting, could lead to an almost symmetric DOS in an InGaAsP DWELL structure. We calculate a total integrated valence DOS of 24×10^{11} cm^{-2} within 50 meV of the VB maximum, compared to an integrated conduction DOS of 8.5×10^{11} cm^{-2} within 50 meV of the band edge when the dashes cover 40% of the well area. The calculated integrated valence and conduction DOS become equal over this energy range when the dashes cover less than 20% of the well area. This indicates that the quasi-Fermi levels for CBs and VBs should progress at very similar rates out of the band gap with increasing carrier injection, close to the ideal case. The introduction of p doping may then have a weaker influence on the differential gain in an InAs/InP DWELL laser compared to conventional quantum well and dot devices. We shall address this matter in further work.

Having established the key features of the band structure in InGaAsP QD lasers, we now investigate the threshold characteristics of a DWELL device similar to that of Fig. 3. We measure the facet emission and the SE emitted through a window in the substrate of this second device, with constant coupling efficiency. From the facet emission, we measure the total threshold current I_{th} and evaluate the external differential quantum efficiency η_d. We use the integrated SE to determine the radiative component I_{rad} of the threshold current by assuming that the current is radiative below 100 K and can be normalized to the total threshold current. Figure 4 shows the measured temperature dependence of I_{th} and of I_{rad} for the DWELL sample (filled data points) and the slope efficiency η_d normalized to its maximum value η_{max}, as open circles. Above 100 K, the threshold current and its radiative

component diverge significantly, due to the onset of temperature-dependent nonradiative current paths and $\eta_d/\eta_{\max}$ decreases significantly above 150 K. The two temperature thresholds suggest the presence of two different temperature-dependent loss mechanisms. The diverging I_{th} and I_{rad} have been reported in other 1.55 μm lasers with quantum well[9] and quantum dot active regions, where optical analysis[9] and pressure measurements[9,10] revealed Auger recombination to be the dominant recombination path. Measurements we have undertaken using the optical analysis method in Ref. 9 support that Auger recombination is also a significant loss mechanism in the devices considered here.[13] We have also analyzed the SE at room temperature from the barrier material around laser threshold. We find that the barrier emission does not fully clamp at laser threshold, indicating the presence of a current leakage path, which contributes to the measured decrease in η_d.

In summary, we have shown that InGaAsP quantum DWELL devices have a band structure that comprises a well-like CB and dashlike VB structure. This difference in confinement dimension, combined with the large strain-induced VB splitting can lead to an almost symmetric DOS in an InGaAsP-based quantum dash laser, something which it has not previously proved possible to achieve, even in highly strained quantum well structures. In addition, the combination of strain and dash shape leads to a significant gain enhancement for light polarized along the (1-10) direction. Nevertheless, experimental measurements show that the introduction of a quantum dash active region does not significantly modify the loss mechanisms compared to a conventional quantum well device as nonradiative current paths are the dominant contribution to the room temperature threshold current and its temperature dependence. Despite the continued presence of these losses, the band structure in the optimized DWELL design leads to a T_0 up to 80 K[2], which is better than conventional GaInAsP multiquantum well[9] and QD (Ref. 10) lasers ($T_0 \approx 50$ K) of significant benefit for telecom laser applications.

We thank R. Fehse, D. P. Williams, R. J. Manning, G. Huyet, and A. R. Adams for useful discussions. This work was supported by ZODIAC IST European project and by Science Foundation Ireland.

[1] M. Sugawara, N. Hatori, M. Ishida, H. Ebe, Y. Arakawa, T. Akiyama, K. Otsubo, T. Yamamoto, and Y. Nakata, J. Phys. D: Appl. Phys. **38**, 2126 (2005).
[2] F. Lelarge, B. Dagens, J. Renaudier, R. Brenot, A. Accard, F. van Dijk, D. Make, O. Le Gouezigou, J. G. Provost, F. Poingt, J. Leandreau, O. Drisse, E. Derouin, B. Rousseau, F. Pommereau, and G.-H. Duan, IEEE J. Sel. Top. Quantum Electron. **13**, 111 (2007).
[3] A. Andreev, J. Downes, D. Faux, and E. O'Reilly, J. Appl. Phys. **86**, 297 (1999).
[4] A. D. Andreev and E. P. O'Reilly, Phys. Rev. B **62**, 15851 (2000).
[5] T. B. Bahder, Phys. Rev. B **41**, 11992 (1990).
[6] Y. Zhang, Phys. Rev. B **49**, 14352 (1994).
[7] E. P. O'Reilly and A. R. Adams, IEEE J. Quantum Electron. **30**, 366 (1994).
[8] R. H. Wang, A. Stintz, P. M. Varangis, T. C. Newell, H. Li, K. J. Malloy, and L. F. Lester, IEEE Photonics Technol. Lett. **13**, 767 (2001).
[9] A. F. Phillips, S. J. Sweeney, A. R. Adams, and P. J. A. Thijs, IEEE J. Sel. Top. Quantum Electron. **5**, 401 (1999).
[10] N. F. Massé, E. Homeyer, I. P. Marko, A. R. Adams, and S. J. Sweeney, Appl. Phys. Lett. **91**, 131113 (2007).
[11] M. Silver and E. P. O'Reilly, IEEE J. Quantum Electron. **31**, 1193 (1995).
[12] M. Mexis, P. M. Smowton, and P. Blood, Semicond. Sci. Technol. **22**, 1298 (2007).
[13] S. Heck and S. Osborne (unpublished).